Non-Newtonian Blood Flow through Stenosed Coronary Arteries

BENCHAWAN WIWATANAPATAPHEE
Department of Mathematics
Mahidol University
Bangkok 10400
THAILAND

SOMKID AMORNSAMANKUL
Department of Mathematics and Statistics
Curtin University of Technology
Perth, Western Australia 6845
AUSTRALIA

YONG-HONG WU
Department of Mathematics and Statistics
Curtin University of Technology
Perth, Western Australia 6845
AUSTRALIA

YONGWIMON LENBURY
Department of Mathematics
Mahidol University
Bangkok 10400
THAILAND

Abstract:- In this paper, a mathematical model is developed to simulate the flow of blood through stenosed coronary arteries taking into account of arterial wall deformation under pulsatile flow condition. The flow of blood through the lumen region is governed by the continuity equation and the Navier-Stokes equations, while blood flow through the poro-elastic wall is described by the Brinkman equations. The deformation of coronary arteries is modelled by the equations of classical elastodynamics. The velocity field, the pressure, the wall shear stress and the deformation of the arterial wall are computed in a fully coupled manner through the use of the fluid-structure interaction condition. The influences of the severity of stenosis on blood flow and wall shear stresses are investigated.

Key–Words:- Mathematical modelling, blood flow, stenosis, coronary artery, poro-elastic wall, finite element method.

1 Introduction

Cardiovascular disease is one of the major causes of death in developed countries. Most of the cases are associated with some form of abnormal blood flow in stenotic arteries. When the coronary artery is affected by a stenosis, critical flow conditions occur, such as flow separation, high wall shear stress and wall compression, which are believed to be the significant factors at the onset of coronary heart diseases. In recent years, surgical treatments of cardiovascular diseases have been developed rapidly, and coronary artery bypass grafting (CABG) has been widely used for patients with severe stenosis. A large number of bypass grafts are implanted worldwide each year. However, up to 25 percents of the grafts fail in one year and up to 50 percents fail in ten years after surgery. Today, it has been recognized that one of the most important determinations in a successful bypass operation is the information of the rheological behavior of blood, the flow speed, the pressure distribution, the wall shear stress in the stenotic artery, and the wall deformation in cardiac cycles.

In order to understand the pathogenesis of coronary diseases, a number of in-vivo and vitro experiments have been conducted using animal models. Due to the difficulty in determining the critical flow conditions for both in-vivo and vitro experiments, the exact mechanism involved is not well understood. On the other hand, mathematical modelling and numerical simulation can lead to better understanding of the phenomena involved in vascular diseases. Thus, over the last two decades, various mathematical models based on the finite element method have been proposed to describe the rheological behavior of blood in stenotic arteries. However, some of the studies describe the fluid flow without taking into account of the motion of the arterial wall, while some others concentrate on the behavior of the structure without taking into account of the fluid flow [9, 8, 4, 7].

It is well established that the fluid-structure interaction determines the behavior of blood flow through arteries. Recently, various studies have focused on the coupled fluid flow - arterial wall deformation problem [2, 5, 6, 3]. Pontrelli [5] proposed a quasi one-dimensional model based on the finite difference

method to describe the wave propagation disturbance due to prosthetic implantation and to investigate the effect of changes in elasticity properties along the vessel. Chahboune and Crolet [2] proposed a two-dimensional mathematical model and a numerical algorithm based on the finite element method for the fluid-structure interaction during the cardiac cycles. The model is used to couple the flow of blood with the motion of the arterial wall of the left ventricle. Gerbeau el al. [3] proposed a three-dimensional model and a numerical algorithm to simulate the fluid-structure interaction in large compliant vessels where large displacement occurs but the biological interpretation of the results are not given. So far, none of the models seems to be completely satisfactory for all kinds of flow regimens.

In this study, we consider the flow of blood through coronary arteries with an unsymmetrical stenosis. Fig. 1 shows the angiogram of such a stenosed coronary artery. A mathematical model is developed to study unsteady state blood flow through a stenotic artery and the deformation of the arterial wall in a cardiac cycle. Human blood is considered as an incompressible non-Newtonian fluid and the arterial wall is modelled as a poro-elastic material. Using three different geometry domains of a straight tube with three different size of stenosis, 25%, 50% and 65%, numerical simulations based on the finite element method are carried out for the flow field, pressure field, internal wall shear stress and the wall deformation in a cardiac cycle. Dependence of the flow field on the severity of stenosis and wall-interaction will be discussed.

2 Mathematical Model

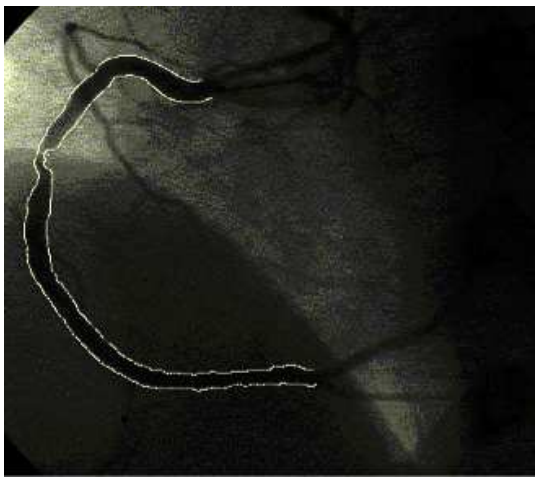

Figure 1: The right coronary artery with stenosis.

The arterial wall consists of three embedded layers including the tunica intima, the tunica media and the adventitia. The innermost layer is the tunica intima which consists of a thin layer of endothelial cells, connective tissue and basement membrane. The middle layer is the tunica media which comprises the smooth muscle cells and a continuous interstitial fluid phase of proteoglycan and collagen fiber. The outermost layer is the adventitia which is made up mostly of stiff collagenous fibers having an elastic modulus of $10^8 - 10^9\ dyn/cm^2$. Blood is transported mainly through the artery lumen but some could be transported through the wall layers. To make the model simple and more tractable, the entire arterial wall is assumed as one poro-elastic layer.

The model in this study uses two coordinate systems. One is a fixed mesh system Ω^F, in which the fluid model in the lumen region is solved. Another system is a moving mesh $\Omega^S(t)$, corresponding to the deformed geometry of the structure, in which the fluid model in the arterial wall is solved. Blood is assumed to be an incompressible non-Newtonian fluid. The non-Newtonian Carreau model is used to determine the viscosity of blood. Blood flow in the lumen region is governed by the continuity equation and the Navier-Stokes equations, while blood flow in the porous wall is described by the Brinkman equations. The wall deformation is modelled by the equations of classical elastodynamics. The velocity fields $\mathbf{u}$ in the luminal channel and $\mathbf{v}$ in the wall and the displacement $\mathbf{d}(\mathbf{x}, t)$ of the arterial wall are computed in a fully coupled manner through the use of the fluid-structure interface condition.

2.1 Continuum Model of Human Blood

Human blood consists of plasma fluid, red blood cells, white blood cells and thrombocyte. The blood plasma is made up of about 90-95% water and contains numerous dissolved materials such as proteins, lipoproteins and ions by which nutrients and wastes are transported. The elements of blood seem to be continuous, with no empty space between the cells. Blood can therefore be assumed as a continuum medium. The small semisolid particles of red blood cells create the viscosity of blood. When the red blood cells clump together into larger particles at low shear rate, the non-Newtonian behavior becomes most evident. It has been generally accepted that when the shear rate is greater than 100 s^{-1} [1], human blood behaves as an incompressible Newtonian fluid and thus the stress - deformation rate relations are described by the Newtonian model :

$$\sigma_{ij}^F = -p^F \delta_{ij} + 2\mu D_{ij}, \qquad (1)$$

where μ is the blood viscosity and D denotes the rate of deformation tensor

$$D_{ij} = \frac{1}{2}(u_{i,j} + u_{j,i})$$

However, when the shear rate is lower than 100 s^{-1}, blood behaves as a non-Newtonian fluid and the stresses depend nonlinearly on the deformation rate. The stresses are related to the deformation rate by

$$\sigma_{ij} = -p^F \delta_{ij} + 2\mu(\dot{\gamma}) D_{ij}, \quad (2)$$

which is similar to the Newtonian model except that the viscosity is a function of shear rate instead of a constant. In different non-Newtonian models, the relation between the viscosity μ_n and the shear rate $\dot{\gamma} = \sqrt{2\mathbf{D} : \mathbf{D}}$ is different. The Carreau model used in this work, $\mu_n = \mu_\infty + (\mu_0 - \mu_\infty)[1 + (\lambda\dot{\gamma})^2]^{(n-1)/2}$ for the constant values of μ_0, μ_∞, λ and n.

2.2 Governing field equations for blood flow

In the luminal region Ω^F, the equations governing the flow of blood include the constitutive equation (2), and the continuity equation as well as the stress equations of motion as detailed below

$$u_{i,i} = 0, \quad (3)$$

$$\rho^F \left(\frac{\partial u_i}{\partial t} + u_j u_{i,j} \right) = \frac{\partial \sigma^F_{ji}}{\partial x_j} + F^F_i, \quad (4)$$

where ρ^F denotes the blood density which is $1.06g\ cm^{-3}$, u_i represents the component of velocity vector in the ith direction, and F^F is the volume force acting on the fluid.

In the arterial wall Ω^S, blood flow is described by the following continuity equation and the Brinkman equations,

$$v_{i,i} = 0, \quad (5)$$

$$\rho^F \frac{\partial v_i}{\partial t} + \frac{\mu}{\kappa} v_i = -p^S_i + (\mu(v_{i,j} + v_{j,i}))_{,j} + F^S_i, \quad (6)$$

where μ denotes the viscosity in porous layer, κ is permeability, v_i represents the component of velocity vector in the ith direction, p^S denotes pressure, and F^S is the body force acting on the fluid in the wall.

2.3 Governing field equations for arterial wall deformation

The arterial wall is assumed as an elastic material. During a cardiac cycle, blood pressure acting on the inner wall surface varies with time, and thus the arterial wall deformation is a function of time. The dynamic wall deformation can be modelled by the equations of classical elastodynamics:

$$\rho^s \frac{\partial^2 \mathbf{d}}{\partial t^2} = \mu \nabla^2 \mathbf{d} + (\lambda + \mu) \nabla(\nabla \cdot \mathbf{d}) \quad (7)$$

where ρ^s is the density of the structure, $\mathbf{d}$ denotes the displacement vector, λ and μ are the Lamé constants which are related to the material Young's modulus E and Poisson's ratio ν by

$$\lambda = \frac{E\nu}{(1+\nu)(1-2\nu)}, \mu = \frac{E}{2(1+\nu)}.$$

2.4 Boundary and interface conditions

To specify the boundary conditions for the blood flow, we consider precisely the blood flow mechanism. The heart is a two-step pump: first the atria, then the ventricles contract. The heart ejects and fills with blood in alternating cycles known as systole and diastole. Blood is ejected from the left ventricle into the arterial system during systole. The heart rests during diastole in which no blood is ejected. The cyclic nature of the heart pump creates pulsatile conditions in all the arteries. The pulsatile characteristic of pressure varies in different part of the arterial system.

Ignoring the variation in different cardiac cycles, the pulsatile pressure and flow rate are given by

$$p(t) = p(t + nT)$$

and

$$Q(t) = Q(t + nT),\ n = 0, \pm 1, \pm 2, \ldots.$$

Mathematically, a periodic function can be expressed as a Fourier series. Based on a typical set of data, we obtain the following Fourier series representations

$$Q(t) = \bar{Q} + \sum_{n=1}^{5} \alpha^Q_n cos(\frac{2n\pi t}{T} - \theta^Q_n) \quad (8)$$

and

$$p_0(t) = \bar{p} + \sum_{n=1}^{5} \alpha^p_n cos(\frac{2n\pi t}{T} - \theta^p_n), \quad (9)$$

where $\bar{Q} = 59.09\ cm^3/min$ and $\bar{p} = 122.5\ mmHg$ are respectively the mean flow rate and mean pressure, T is the cardiac period, and the values of α^Q_n, α^p_n, θ^Q_n and θ^p_n are listed in Table 1.

We therefore impose a pulsatile flow rate condition on the inlet boundary and a corresponding pulsatile pressure condition on the outlet boundary of the

Table 1: Values of parameters used in computation

n	α_n^Q	θ_n^Q	α_n^p	θ_n^p
1	17.28	2.256	-21.740	-0.406
2	-34.91	-0.226	-9.088	0.202
3	-16.11	1.228	4.771	-0.633
4	11.70	4.882	2.035	-4.315
5	6.64	-0.074	0.768	3.932

computation region. The boundary conditions for the velocity and pressure fields thus include both Dirichlet type and Neumann/Robin type, i.e, for $i, j = 1, 2, 3$

$$u_1 = \bar{u}_0(t) = \frac{Q(t)}{A}, \quad u_2 = u_3 = 0 \quad \text{on } \partial\Omega_{in}^F$$
$$p = p_0(t), \quad (\mu_n(u_{i,j} + (u_{j,i})) \cdot \mathbf{n} = 0 \quad \text{on } \partial\Omega_{out}^F \tag{10}$$

where A denotes the inlet cross-section area of the artery, $Q(t)$ is the pulsatile flow rate, $p_0(t)$ represents the pulsatile pressure.

On the interface between the lumen and the arterial wall $\Gamma^{F/S}$, the expression for the velocity must be continuous across the interface. We thus set

$$\mathbf{v} = \mathbf{u} = \frac{\partial \mathbf{d}}{\partial t}. \tag{11}$$

The movement of the inflow and outflow boundaries $\partial\Omega_{in}^S$ and $\partial\Omega_{out}^S$ of the structure is assumed to be restricted in all directions,

$$\mathbf{d}(\mathbf{x}, t) = 0. \tag{12}$$

3 Numerical results and discussion

From section 2, the boundary value problem governing the fluid-structure interaction in stenotic arteries is:

BVP : Find $\mathbf{u}, \mathbf{v}, p^F, p^S$ and $\mathbf{d}$ such that the field equations (3)–(7) are satisfied in the computation domain, and all boundary conditions are satisfied.

A numerical algorithm based on the finite element method has been developed to solve the problem. The feature of the algorithm include discretization in space by the Galerkin finite element method, use of different function spaces for velocity and pressure, coupling of velocity with wall deformation on the fluid-solid interface, and time integration with variable time step.

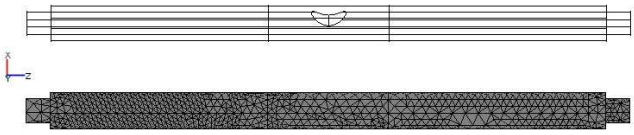

Figure 2: The 3-D geometry of the 50% stenotic tube and its finite element mesh.

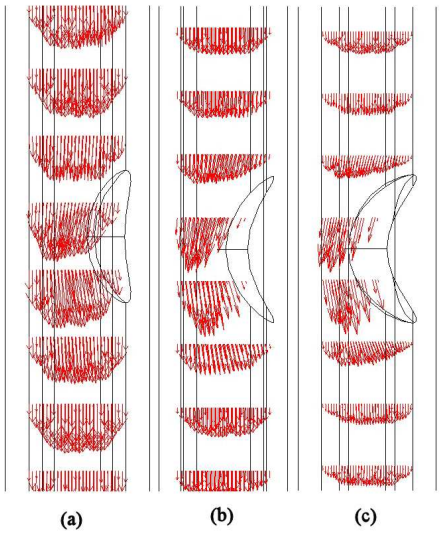

Figure 3: Vector profiles of the velocity field in the luminal channel at the peak of systole: (a) 25% stenosis, (b) 50% stenosis, (c) 65% stenosis.

The numerical technique is then used to study the flow of blood through a stenotic artery. In this study, we examine three cases of stenotic arteries with 25%−, 50%− and 65%−area severity respectively. The part of the artery to be examined is approximated as a straight tube with length of 5 cm. The diameter of the artery lumen is 0.210 cm, and the thickness of the arterial wall is 0.05 cm. There is a stenosis with spherical curvature in the middle part on one side of the internal wall as shown in Fig.2. The three-dimensional tubes having 25% 50% and 65%-area severity are respectively discretized into 10,092 tetrahedron elements with 77,451 degrees of freedom (velocity and pressure), 12,700 tetrahedron elements with 96,354 degrees of freedom, and 8,151 tetrahedron elements with 62,574 degrees of freedom. The solutions were computed for 5 cardiac cycles to ensure reproducibility of the pulsatile characteristic flow. In all the three cases, the minimum time step is taken to be $\triangle t_{min} = 0.001s$, while the maximum time step is $\triangle t_{max} = 0.01s$.

To determine the inlet pulsatile flow rate and outlet pulsatile pressure, the parameters listed in Table 1

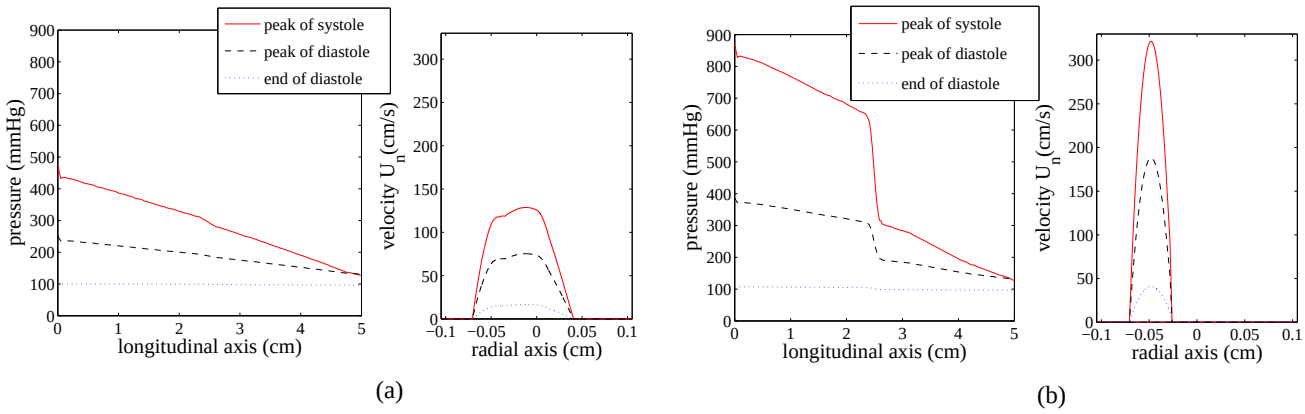

Figure 4: Distribution of pressure along the longitudinal line and variation of blood speed along the throat line of the stenosis for three different cases of stenosis area severity: (a) 25% and (b) 65% -area severity

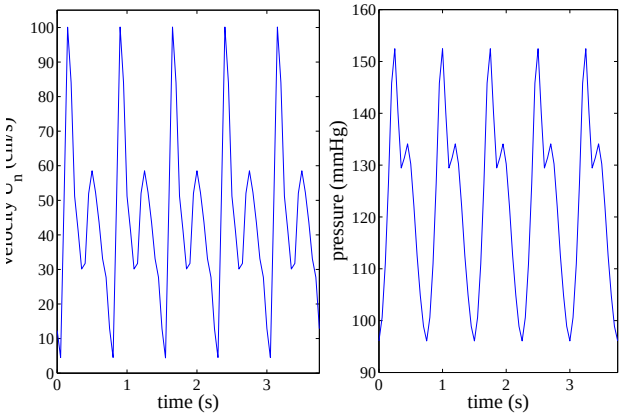

Figure 5: Variations of pulsatile velocity and pulsatile pressure with time at a point (0,0,5) on the exit surface of the 65% stenotic artery.

are used. Fig. 3 depicts the velocity field in the luminal channel at the peak of systole in the Oxy plane for the 25%, 50%, 65% stenotic tubes. The plot clearly shows the flow pattern. In upstream from the stenosis, the velocity profile in the flow direction is parabolic and the flow passes through the stenosis at jet speed, especially at the throat of the stenosis.

The relation between blood pressure and blood velocity is demonstrated in Fig. 4. These figures illustrate the pressure distribution along a longitudinal line and the mean flow of blood at the throat line during the systolic period. It shows that the pressure drops dramatically near the stenosis site and creates a jet flow at the throat of the stenosis. The case with larger stenosis causes larger pressure drop around the stenosis and consequently leads to higher speed in the stenosis area.

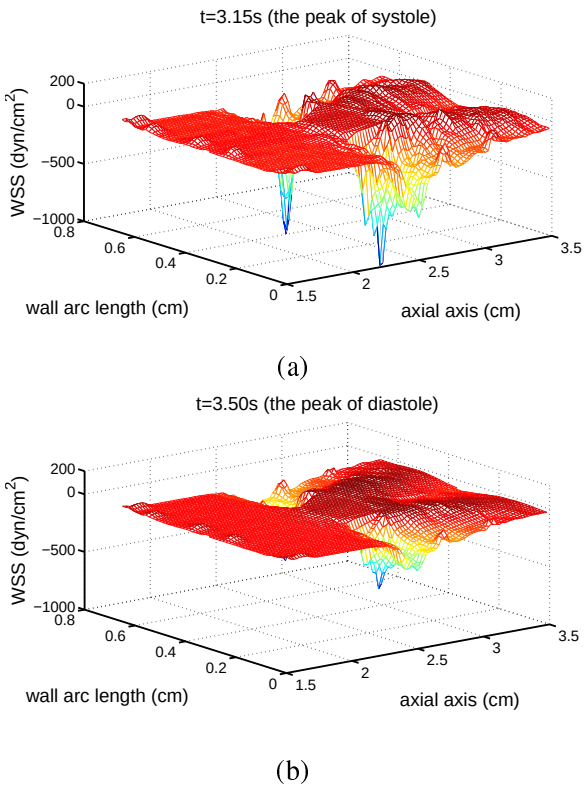

Figure 6: Surface plot of wall shear stresses (WSS) for the 65% stenotic artery: (a) at the peak of systole $t = 3.15s$ and (b) at the peak of diastole $t = 3.50s$.

Figs. 5 shows the pulsatile characteristic of blood flow. To capture the effect of wall-interaction on wall shear stresses, we investigate the models with 65%-area severity at the peak of systole and at the peak of diastole. The solutions are plotted on the plane representing the wall surface where the stenosis is located at the center. The results show that in the model with the porous wall, at the peak of systole the wall shear stress around the stenosis site varies between -965 and -200 dyn/cm^2, and at the peak of diastole it varies between -510 and -100 dyn/cm^2 as shown in Figs. 6.

4 Conclusions

The presented work is carried out to couple the flow of blood with the deformation of blood vessels. The convective-diffusive transport of blood in the luminal channel and in the arterial porous wall as well as the deformation of the stenosed coronary artery have been studied numerically using a three-dimensional mathematical model and a numerical technique based on the finite element method. The results obtained from the vessel models having 25%, 50% and 65%-area severity show that blood pressure drops dramatically around the stenosis site and creates a jet flow at the throat of the stenosis and that a larger stenosis leads to a higher pressure jump, higher blood speeds around the stenosis site.

Acknowledgements: This work was supported by the 2005 Australia Endeavour Cheong Kong Award for the first author to undertake research at Curtin University of Technology, Western Australia from April to October 2005. The first author also was supported by the Mahidol University through Mahidol Research Fund.

References:

[1] Michael Bonert, Jerry G. Myers, Stephen Fremes, James Williams and C. Ross Ethier, A Numerical Study of Blood Flow in Coronary Artery Bypass Graft Side-to-Side Anastomoses, In *Annals of Biomedical Engineering*, Vol. 30, 2002, pp. 599–611.

[2] B. Chahboune and J. M. Crolet, Numerical simulation of the blood-wall interaction in the human left ventricle, *The European Physical Journal Applied Physics*, Vol. 2, 1998, pp. 291–297.

[3] Jean-Frédéric Gerbeau, Marina Vidrascu and Pascal Frey, Fluid-structure interaction in blood flows on geometries based on medical imaging, *Computers and Structures*, Vol. 83, 2005, pp. 155–165.

[4] Hun Jung, Jong Wook Choi and Chan Guk Park, Asymmetric flows of non-Newtonian fluids in symmetric stenosed artery, *Korea-Australia Rheology Journal*, Vol. 16, 2004, pp. 101–108.

[5] Giuseppe Pontrelli, Nonlinear problems in arterial flows, *Nonlinear Analysis*, Vol. 47, 2001, pp. 4905–4915.

[6] Giuseppe Pontrelli, A Multiscale Approach for Modelling Wave Propagation in an Arterial Segment, *Computer Methods in Biomechanics and Biomedical Engineering*, Vol. 7, 2004, pp. 79–89.

[7] B. R. Simon, M. V. Kaufmann, M. A. McAfee and A. L. Baldwin, Finite Element Models for Arterial Wall Mechanics, *Journal of Biomechanical Engineering*, Vol. 115, 1993, pp. 489–496.

[8] D. Kim Stangeby and C. Ross Ethier, Computational Analysis of Coupled Blood-Wall Arterial LDL Transport, *Journal of Biomechanical Engineering*, Vol. 124, 2002, pp. 1–8.

[9] Shigeru Tada and John M. Tarbell, Interstitial flow through the internal elastic lamina affects shear stress on smooth muscle cells in the artery wall, *The American Journal of Physiology - Heart and Circulatory Physiology*, Vol. 278, 2000, pp. 1589–1597.